



25 **ABSTRACT**

26 The post-acute sequelae of COVID-19 (PASC) poses a significant health challenge in the post-  
27 pandemic world. However, the underlying biological mechanisms of PASC remain intricate and elusive.  
28 Network-based methods can leverage electronic health record (EHR) data and biological knowledge to  
29 investigate the impact of COVID-19 on PASC and uncover the underlying biological mechanisms. This  
30 study analyzed territory-wide longitudinal electronic health records (from January 1, 2020, to August  
31 31, 2022) of 50296 COVID-19 patients and a healthy non-exposed group of 100592 individuals to  
32 determine the impact of COVID-19 on disease progression, provide molecular insights, and identify  
33 associated biomarkers. We constructed a comorbidity network and performed disease-protein mapping  
34 and protein-protein interaction network analysis to reveal the impact of COVID-19 on disease  
35 trajectories. Results showed disparities in prevalent disease comorbidity patterns, with certain patterns  
36 exhibiting a more pronounced influence by COVID-19. Overlapping proteins elucidate the biological  
37 mechanisms of COVID-19's impact on each comorbidity pattern, and essential proteins can be  
38 identified based on their weights. Our findings can help clarify the biological mechanisms of COVID-  
39 19, discover intervention methods, and decode the molecular basis of comorbidity associations, while  
40 also yielding potential biomarkers and corresponding treatments for specific disease progression  
41 patterns.

42  
43 **Keywords:** network science, comorbidity, network medicine, post-acute sequelae of COVID-19

44  
45 **Word count: 4513 (5598 including figures and tables)**

46 **The accurate identification of comorbidity patterns associated with elevated COVID-19**  
47 **infection risk is essential for effective medical resource allocation, prioritizing care, and**  
48 **supporting patient recovery. This study delved into the biological mechanisms underlying post-**  
49 **acute sequelae of COVID-19 by analyzing the comorbidity network. Key proteins and**  
50 **significant biological pathways were identified through Protein-Protein Interaction network**  
51 **analysis and Gene Ontology enrichment analysis. These insights not only contribute to**  
52 **understanding the fundamental mechanisms of post-acute sequelae but also hold potential as**  
53 **biomarkers and therapeutic targets, laying the groundwork for the development and**  
54 **repurposing of drugs to benefit COVID-19 patients.**

## 55 56 INTRODUCTION

57 The global pandemic of Coronavirus Disease 2019 (COVID-19), caused by severe acute respiratory  
58 syndrome coronavirus 2 (SARS-CoV-2) infection, has impacted billions of people, resulting in millions  
59 of deaths, and leaving tens of millions suffering from persistent symptoms and signs after the acute  
60 phase of COVID-19<sup>1</sup>. This phenomenon, referred to as post-acute sequelae of COVID-19 (PASC), is  
61 gradually coming to an end<sup>2,3</sup>. PASC exhibits heterogeneous manifestations and severity<sup>4</sup>, impacting  
62 various organ systems including cardiovascular<sup>5,6</sup>, mental<sup>7</sup>, metabolic<sup>8</sup>, and renal systems<sup>9</sup>. However,  
63 the underlying biological mechanisms of PASC remain intricate and elusive.

64  
65 Current research on the potential biological mechanisms of COVID-19 and PASC primarily involves  
66 small patient cohorts and concentrates on the relationship between COVID-19 and diseases in specific  
67 systems or organs individually<sup>2,10-12</sup>. Investigations involving large patient cohorts and associations  
68 between COVID-19 and diseases across multiple organs and systems can aid in uncovering the  
69 biological mechanisms of multimorbidity present in PASC and pre-existing diseases influenced by  
70 COVID-19. Comorbidity and multimorbidity<sup>13</sup> refer to the co-occurrence of two or more diseases in an  
71 individual. If the frequency of co-occurrence of diseases exceeds the frequency of disease combinations  
72 selected by chance, multimorbidity exists among these diseases. Research on multimorbidity  
73 associations with PASC has shown that pre-existing multimorbidity may drive PASC<sup>10,14</sup>. The  
74 underlying mechanisms of multimorbidity are complex, potentially involving shared genetic or

75 environmental factors or resulting from the treatment or intervention for one disease leading to the  
76 development of another<sup>14</sup>. Studies on multimorbidity relations in PASC have considered the influence  
77 of demographic factors<sup>15,16</sup> like sex, age, race, COVID-19 vaccine injection, and patient electronic  
78 health records (EHR) diseases. However, the underlying biological mechanisms of these multimorbidity  
79 relations influenced by COVID-19 remain unclear.

80

81 Our research utilized territory-wide EHR data from the Hong Kong Hospital Authority to investigate  
82 the impact of COVID-19 on PASC. We employed network-based methods to assess the influence of  
83 COVID-19 on multimorbidity across multiple organs and systems in PASC. Individuals with specific  
84 pre-existing diseases may have a higher risk of developing certain diseases included in PASC due to  
85 the effects of COVID-19. To explore the underlying mechanisms of these particular multimorbidity  
86 relations, we incorporated biological knowledge from the protein-protein interaction (PPI) network<sup>17</sup>  
87 and Gene Ontology (GO) enrichment analysis<sup>18</sup> to identify the most affected and essential proteins that  
88 could serve as potential targets for future interventions, such as preventive measures.

89

## 90 **METHODS**

### 91 **Study design and population**

92 All electronic datasets included in this research are from the Hong Kong Hospital Authority (HKHA)  
93 database. Based on the COVID-19 record (based on rapid antigen test [RAT] or polymerase chain  
94 reaction [PCR] test in throat swab, nasopharyngeal aspirate, or deep throat sputum specimens), patients  
95 are divided into two groups: exposure and non-exposed groups. (Supplementary Figure 4)

96

97 For the exposure group, the diagnose records within 730 days before COVID-19 and 180 days after  
98 COVID-19 are retained. We then exclude all diagnose records within 28 days (acute-phase of infection)  
99 after COVID-19. For each individual, diseases appearing before COVID-19 were considered as pre-  
100 existing diseases, and new emerging diseases appearing after COVID-19 were considered as post-  
101 infection diseases.

102

103 For the non-exposed group, we applied the same procedure to identify the pre-existing and post-  
104 infection diseases for each individual by treating the date 180 days before the last record date as the  
105 simulated COVID-19 infection date.

106  
107 To investigate the influence of COVID-19 on PASC, we compared the differences in comorbidity  
108 patterns between the exposure group (people with first COVID-19 in 2022) and the non-exposed group  
109 (people without COVID-19). To ensure a fair comparison, we employed propensity score matching<sup>19</sup>  
110 to select a non-exposed group with pre-existing disease records similar to the exposure group. In the  
111 matching process, we considered not only individual EHR data denoted by 3-digital ICD-9 codes from  
112 the baseline period, but also demographic data (age, sex) and vaccine information (vaccine number).  
113 After matching, we calculated the standardized mean difference (SMD) to quantify the balance for each  
114 confounder. An SMD value below 0.1 serves as a threshold to determine whether the confounder is  
115 well-balanced.

### 116 117 **Propensity Score Matching**

118 We included all disease related 3-digital ICD-9 CM codes from pre-existing diseases in both non-  
119 exposed and exposure groups. Each appearing ICD-9 code serves as a feature in the Propensity Score  
120 Matching. The number of vaccinations received prior to COVID-19 is included as a feature. For each  
121 individual in the exposure group, we select the two nearest neighbors from the non-exposed group based  
122 on the processed propensity score, which is obtained by applying a logit function. After propensity  
123 score matching, the COVID-19 and non-exposed groups include 50296 and 100592 patients  
124 respectively, from 58753 in the COVID-19 group and 488670 in the non-exposed group. (details are  
125 shown in Supplementary Table 2) In the following comorbidity patterns' coefficient computation part,  
126 we considered patients with at least one new disease and excluded patients without new post-infection  
127 diseases.

### 128 129 **Comorbidity network construction**

130 According to COVID-19 infection date for each individual in the exposure group (simulated for the  
131 non-exposed group). We first define pre-existing diseases as those diagnosed before COVID-19, and

132 post-infection diseases as new emerging diseases diagnosed >28 days after COVID-19. We generated  
133 disease pairs by selecting the first disease from all pre-existing diseases and the second disease from all  
134 post-infection diseases and applied Pearson correlation coefficient and relative risk to quantify the co-  
135 occurrence of two diseases composing each disease pair.<sup>20</sup> To reduce bias from data and computation  
136 methods, we used both values to identify co-occurring disease pairs combining with chi-square and  
137 fisher exact test.<sup>20</sup> We identified disease pairs appearing in the exposure group with Pearson correlation  
138 coefficient > 0 and relative risk > 1 as comorbidity patterns. To investigate comorbidity patterns  
139 influenced by COVID-19, we selected comorbidity patterns according to the three requirements: (1)  
140 comorbidity patterns are significantly more frequent (Fisher exact test or chi-square test, p-value < 0.05)  
141 in the exposure group than in the non-exposed group. (2) the count number of each comorbidity pattern  
142 in the exposure group is at least 10. (3) the Pearson correlation coefficient and relative risk of each  
143 comorbidity are larger in the exposure group than in the non-exposed group. Selected comorbidity  
144 patterns are used for comorbidity network construction. In the comorbidity network, each node  
145 represents a disease, and each directed edge from a pre-existing disease to a post-infection disease  
146 represents a comorbidity pattern indicating higher prevalence in the exposed group than in the non-  
147 exposed group. For instance, an edge like (disease A, disease B) suggests that individuals with pre-  
148 existing disease A face an elevated risk of developing disease B following COVID-19, compared to  
149 those without COVID-19 exposure. The difference in Pearson correlation coefficients and relative risk  
150 for each comorbidity pattern between exposure group and non-exposed group are considered as  
151 additional attributes for edges.

152

153 Relative Risk denoted by  $RR_{ij}$  represents the relative risk between disease  $i$  and disease  $j$ .  $C_{ij}$  is the  
154 number of co-occurrence incidences of disease  $i$  and disease  $j$ ,  $I_i$  is the number of incidences of disease  
155  $i$ ,  $I_j$  is the number of incidences of disease  $j$ , and  $N$  is the number of patients included in the dataset (for  
156 the non-exposed group and exposure group).

$$157 \quad RR_{ij} = C_{ij}/(I_i I_j / N) \quad (1)$$

158 Pearson correlation is another common method to evaluate the strength of diseases' connection. The

159 Pearson correlation between disease  $i$  and disease  $j$  is denoted by  $\phi_{ij}$ , and the formula is the following:

160 
$$\phi_{ij} = [(N C_{ij}) - I_i I_j] / \text{sqrt}(I_i I_j (N - I_i)(N - I_j)) \quad (2)$$

161

162 Disease pairs with Pearson correlation coefficient  $> 0$  and relative risk  $> 1$  imply that these diseases are  
163 more likely to occur than by chance.

164

### 165 **Protein-Protein Interaction (PPI) network and SARS-CoV-2 human proteins**

166 The protein-protein interaction network used in this study was assembled from 21 public databases by  
167 Barabási<sup>21</sup>. The final interactome used in our study contains 18,505 proteins and 327,924 interactions  
168 between them. For SARS-CoV-2 human proteins, we used related data detected by Gordon<sup>22</sup>. To  
169 quantify the distance between the post-infection and pre-existing diseases, we utilized node-node  
170 distances for each protein pair on the largest connected component of the protein-protein interaction  
171 network, which contains 18446 nodes and 327868 edges. All proteins are represented by their encoded  
172 genes (Entrez ID and Symbol ID).

173

### 174 **ICD code and Gene/Protein association data**

175 Data were derived from the DisGeNET<sup>23,24</sup> database and the OMIM<sup>25,26</sup> dataset. These datasets  
176 encompass information about proteins and diseases, as well as their interrelationships. Utilizing these  
177 datasets, we were able to identify proteins associated with each disease. The distances between diseases  
178 were determined based on the distances between their associated proteins. From the DisGeNET  
179 database and the OMIM dataset, we assigned associated proteins to 537 diseases, each disease identified  
180 by an ICD-9 code and each disease-associated protein identified by its encoded gene (Entrez ID and  
181 Symbol ID).

182

### 183 **Distance Measure**

184 Disease-protein relations are utilized to map each disease, denoted by an ICD-9 code, to the protein-  
185 protein interaction (PPI) networks. Diseases are represented by protein groups, which are sets of  
186 proteins associated with a specific disease. The topological distance between corresponding protein



187 groups in the PPI networks measures the distance between two diseases. A shorter distance between the  
188 protein groups indicates a closer relation between the diseases.

189 For example, if we have a pre-existing disease A and a post-infection disease B, we can map them to  
190 the PPI networks and find their corresponding protein groups. Then, we can calculate the distance  
191 between them as  $d_{AB}$ , where  $d(a, b)$  represents the shortest path from protein a to protein b in the PPI  
192 networks.

$$193 \quad \langle d_{AB} \rangle = \frac{1}{\|B\|} \sum_{b \in B} \min_{a \in A} d(a, b) \quad (3)$$

194 To compute the distance between a pre-existing disease A with COVID-19 and a post-infection  
195 disease B, we need to integrate proteins associated with COVID-19 (denoted by C) and  
196 proteins associated with disease A. The computation formula is as follows:

$$197 \quad \langle d_{AB}^C \rangle = \frac{1}{\|B\|} \sum_{b \in B} \min_{a \in A \cup C} d(a, b) \quad (4)$$

198 The distance change (denoted by  $\Delta d_{AB}$ ) for a pre-existing disease A and a post-infection  
199 disease B with and without the addition of proteins associated with COVID-19 is as follows:

$$200 \quad \Delta d_{AB} = \langle d_{AB} \rangle - \langle d_{AB}^C \rangle \quad (5)$$

202 We also apply the following methods to compute disease distances for sensitivity analysis:

$$203 \quad \langle d_{AB} \rangle = \frac{1}{\|A\| \|B\|} \sum_{b \in B} \sum_{a \in A} d(a, b) \quad (6)$$

## 204 Testing Method

205 We employed two statistical tests, the Chi-square test and the Fisher's exact test, to compare the co-  
206 occurrence frequency of disease pairs between the non-exposed and exposure groups. These tests can  
207 assist us in determining whether a significant association exists between two diseases in the presence  
208 or absence of COVID-19.

209  
210 Among all 537 diseases which have at least one associated protein, for each pre-existing disease, we  
211 treated selected comorbidity patterns as positive samples and generated negative samples (disease pairs  
212 composed of pre-existing disease and other diseases, which are different from selected comorbidity  
213 patterns). Additionally, we utilized the Wilcoxon signed-rank test to compare the changes of protein-



214 protein interaction (PPI) distance before and after the addition of proteins associated with COVID-19  
215 to proteins associated with pre-existing disease between each disease pair in the positive group and all  
216 disease pairs with the same pre-existing disease in the negative group. This test can help us evaluate  
217 whether a significant difference exists in the PPI distance between each disease pair in the positive  
218 group and all disease pairs with the same pre-existing disease in the negative sample group, thereby  
219 indicating the impact of COVID-19 on the relationship between two diseases.

### 221 **Negative Sample for Z-score Compute**

222 For each pre-existing post-infection disease pair, we conduct a permutation test of 1000 repeats to  
223 compute Z-score. We randomly select proteins from the PPI network, and the selected protein groups  
224 are required to have similar node degree distribution to pre-existing disease and post-infection disease  
225 respectively. Distance differences before and after adding proteins associated with COVID-19 as a part  
226 of pre-existing disease associated proteins are also calculated based on the randomly selected protein  
227 groups, and the mean value and standardized deviation of the result are used to compute Z-score for  
228 each pre-existing post-infection disease pair according to the following formula:

$$229 \quad Z_{\Delta d_{AB}} = \frac{\Delta d_{AB} - \mu_r}{\sigma_r} \quad (7)$$

230  $\Delta d_{AB}$  is the distance change of pre-existing post-infection disease pair before and after adding  
231 proteins associated with COVID-19 as a part of pre-existing disease associated proteins.  $\mu_r$  is the  
232 mean value of the distance change from the permutation test,  $\sigma_r$  is the standardized deviation of the  
233 distance change from the permutation test.

### 234 **GO enrichment Analysis**

235 GO terms describe the functions of gene products across three primary aspects: biological process,  
236 molecular function, and cellular component. By conducting GO enrichment analysis, we can pinpoint  
237 the GO terms and crucial genes most impacted by COVID-19, thereby enhancing our understanding of  
238 the disease's underlying biology.<sup>18,27-29</sup> We employed Fisher's exact test for the enrichment analysis  
239 and used the Benjamini-Hochberg procedure to adjust the p-values for multiple testing.<sup>30,31</sup>

240

241 GO Term and Gene Information are from the National Center for Biotechnology Information(NCBI).  
242 These datasets include information on GO terms and the relationships between GO terms, genes, and  
243 proteins. We can also identify proteins associated with each GO term. By utilizing GO enrichment  
244 analysis, we can discover highly influenced GO terms for each disease based on its associated proteins.

245

### 246 **Protein and GO terms Evaluation**

247 The importance of overlapping proteins and GO terms (those associated with both the post-infection  
248 disease and pre-existing disease with COVID-19) is the sum of the coefficients of disease pairs they are  
249 associated with based on TF-IDF metric.<sup>32</sup> We can sort overlapping proteins and GO terms by Relative  
250 Risk (RR), Correlation Coefficient and frequency, respectively. The final index of each item is  
251 determined by the mean index of those three indices. According to the final index, we can identify  
252 important proteins and GO terms.

253

## 254 **RESULTS**

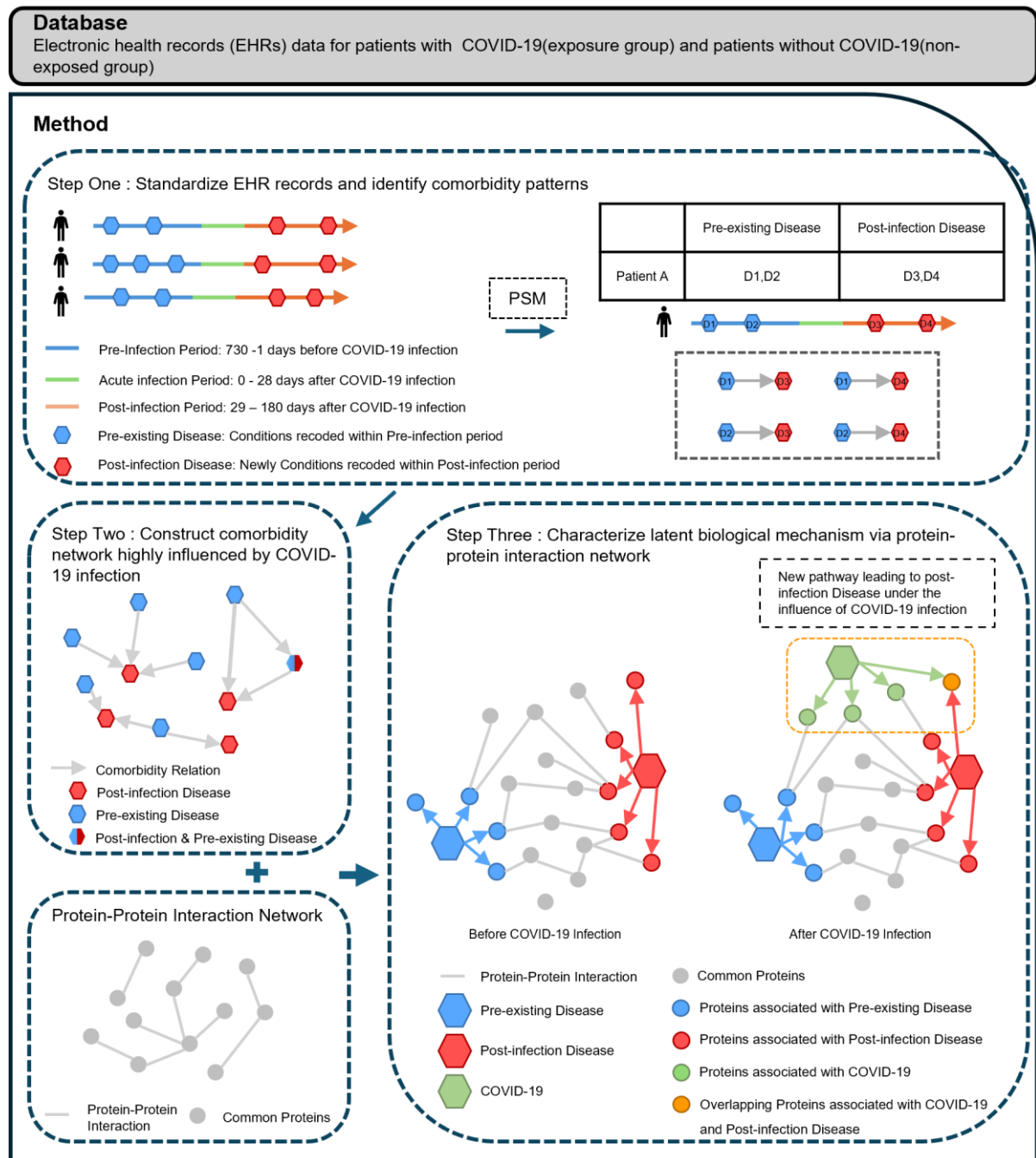
### 255 **Overall pipeline**

256 Using propensity score matching, we construct a non-exposed group (patients without COVID-19  
257 record) and an exposure group (COVID-19 patients) with similar clinical records prior to their  
258 respective first COVID-19 record (simulating infection date for healthy individuals) from January 1,  
259 2020 to August 31, 2022. Then, we construct and analyze the comorbidity network as follows:

- 260 • For each individual, we first define *pre-existing diseases* as those diagnosed within 730 days before  
261 COVID-19, and *post-infection diseases* as new diseases diagnosed in 28 days to 180 days after  
262 COVID-19. We define the *disease pair* as a pair of a pre-existing disease and a post-infection  
263 disease in the exposure group. *Comorbidity patterns* refer to these disease pairs with a positive  
264 Pearson correlation coefficient between pre-existing and post-infection diseases with a relative  
265 risk  $> 1$  (More details are shown in the Method part).
- 266 • We then construct a comorbidity network<sup>33</sup> consisting of these comorbidity patterns and involved  
267 diseases. In our comorbidity network, each node represents a disease. The existence of a directed  
268 edge from the pre-existing disease to the post-infection disease indicates the comorbidity pattern  
269 is significantly more frequent ( $p$ -value  $< 0.05$ , larger Pearson correlation coefficient and relative

270 risk) in the exposure group than in the non-exposed group. The difference in Pearson correlation  
 271 coefficient and relative risk for each comorbidity pattern between the exposure group and the non-  
 272 exposed group are considered as additional attributes for edges.

- 273 • For each comorbidity pattern, as represented by an edge in the comorbidity network, network  
 274 analysis and GO enrichment<sup>18,34,35</sup> analysis were employed for biological pathways discovery by  
 275 utilizing corresponding disease-associated proteins with COVID-19 associated proteins, and  
 276 important proteins and GO terms were identified.



278 **Figure 1. Data curation and analysis pipeline.** To explore the molecular mechanism of Post-Acute  
 279 Sequelae of COVID-19, we stratify patients to the exposure group and the non-exposed group and  
 280 define disease pairs based on their electric health records after propensity score matching (step 1). After  
 281 filtering disease pairs, we construct a comorbidity network based on the correlation coefficient between  
 282 pre-existing and post-infection diseases (step 2). Finally, we utilize the protein-protein interaction  
 283 network to identify potential key proteins and biological pathways in comorbidity patterns under the  
 284 influence of COVID-19 (step 3).

285  
 286 **Study cohorts**

287 Before matching, the dataset comprised 58753 individuals with COVID-19 and 488670 individuals  
 288 without COVID-19 (refer to Supplementary Table 1). Following the matching process (as detailed in  
 289 the Methods section), the exposure group contained 50296 observations, while the non-exposed group  
 290 contained 100592 observations. The median age for the non-exposed group is 65, compared to 66 for  
 291 the exposure group. The non-exposed group was composed of 52.4% males and 47.6% females,  
 292 whereas the exposure group consisted of 52.2% males and 47.8% females. Over 50% of the individuals  
 293 in both groups are aged 60 years or older. Further details regarding specific diseases are shown in  
 294 Supplementary Figure 1 and the SMD of features are shown in Supplementary Table 2. Utilizing the  
 295 electronic health records of each individual in the two groups, we were able to construct a directed  
 296 comorbidity network, which illustrates the disease trajectories before and after COVID-19.

297  
 298 **Table 1. Summary statistics of the dataset.**

	Overall	Non-exposed group	exposure group	
<b>Num</b>	150888	100592	50296	
<b>Vaccine num, n (%)</b>	<b>0 dose</b>	46013 (30.5)	30880 (30.7)	15133 (30.1)
	<b>1 dose</b>	22015 (14.6)	14564 (14.5)	7451 (14.8)
	<b>2 doses</b>	68563 (45.4)	45705 (45.4)	22858 (45.4)
	<b>3 doses</b>	10903 (7.2)	7248 (7.2)	3655 (7.3)
	<b>4 doses</b>	3394 (2.2)	2195 (2.2)	1199 (2.4)
<b>Age, median [Q1,Q3]</b>	65.0 [53.0,76.0]	65.0 [53.0,76.0]	65.0 [53.0,76.0]	
<b>Sex, n (%)</b>	<b>Female</b>	78933 (52.3)	52682 (52.4)	26251 (52.2)
	<b>Male</b>	71955 (47.7)	47910 (47.6)	24045 (47.8)
<b>Num of diseases before COVID-19, mean (SD)</b>	4.0 (3.9)	4.0 (4.0)	3.9 (3.7)	

<b>Num of diseases after COVID-19, mean (SD)</b>		1.8 (1.9)	1.9 (2.0)	1.6 (1.8)
<b>Num of pre-existing diseases before COVID-19 for exposure group and Non-exposed group (simulate), n (%)</b>	<b>1 disease</b>	42406 (28.1)	28405 (28.2)	14001 (27.8)
	<b>2 diseases</b>	30099 (19.9)	20499 (20.4)	9600 (19.1)
	<b>3 diseases</b>	20287 (13.4)	13349 (13.3)	6938 (13.8)
	<b>4 diseases</b>	13823 (9.2)	8951 (8.9)	4872 (9.7)
	<b>more than 5 diseases</b>	44273 (29.3)	29388 (29.2)	14885 (29.6)
<b>Num of post-infection diseases after COVID-19 for exposure group and Non-exposed group (simulate), n (%)</b>	<b>1 disease</b>	64244 (42.6)	42312 (42.1)	21932 (43.6)
	<b>2 diseases</b>	27835 (18.4)	18907 (18.8)	8928 (17.8)
	<b>3 diseases</b>	12900 (8.5)	8898 (8.8)	4002 (8.0)
	<b>4 diseases</b>	7169 (4.8)	4956 (4.9)	2213 (4.4)
	<b>more than 5 diseases</b>	12208 (8.1)	8863 (8.8)	3345 (6.7)
	<b>no disease</b>	26532 (17.6)	16656 (16.6)	9876 (19.6)
<b>Age group, n (%)</b>	<b>0-20</b>	4228 (2.8)	2927 (2.9)	1301 (2.6)
	<b>20-40</b>	14389 (9.5)	9691 (9.6)	4698 (9.3)
	<b>40-60</b>	35999 (23.9)	23778 (23.6)	12221 (24.3)
	<b>60-80</b>	65776 (43.6)	43552 (43.3)	22224 (44.2)
	<b>80+</b>	30496 (20.2)	20644 (20.5)	9852 (19.6)

299

300

### 301 Comorbidity Network Analysis

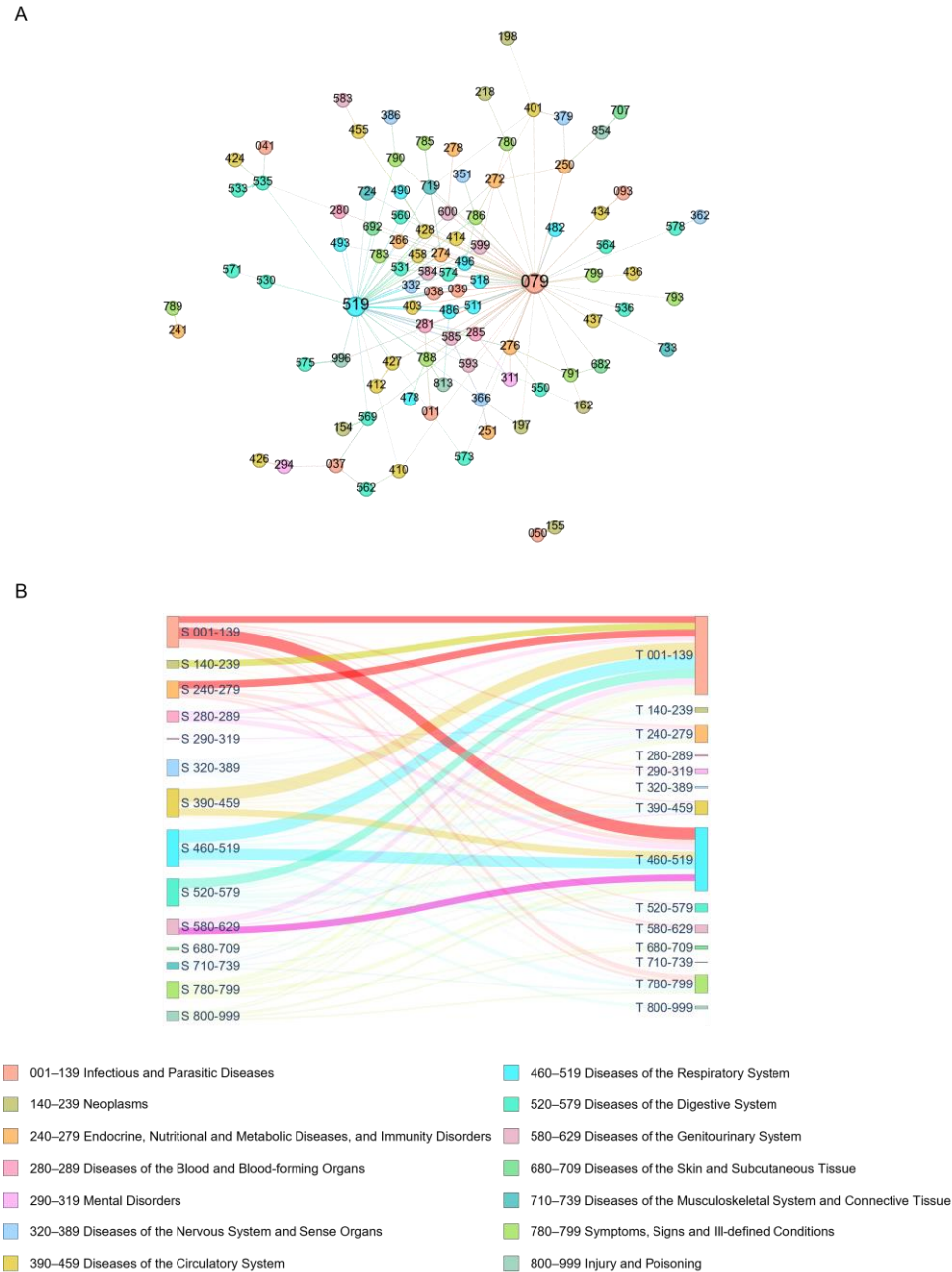
302 Our comorbidity network comprises 96 nodes and 161 edges, representing the comorbidity patterns  
 303 significantly influenced by COVID-19. Nodes are categorized into 14 disease groups according to their  
 304 ICD9 categories. Edges are classified into two groups according to the adjacent nodes: intra-group  
 305 edges (source node and target node in the same disease group), inter-group edges (source node and  
 306 target node in different disease groups).

307

308 Figure 2 (A) (B) depict the constructed comorbidity network and disease group classifications. The  
 309 network is heterogeneously connected, with most disease groups sparsely associated with other disease  
 310 groups and a few disease groups more closely related to some other disease groups. More specifically,  
 311 among all groups, disease group (001–139 Infectious and Parasitic Diseases) and disease group (460–  
 312 519 Diseases of the Respiratory System) have a higher frequency than other disease groups. 079 (Viral  
 313 and chlamydial infection in diseases classified elsewhere and of unspecified site) and 519 (Other  
 314 diseases of respiratory system) are two most frequent diseases among all, indicating that COVID-19  
 315 has the most significant impact on the respiratory system. Additionally, the neural, gastrointestinal and  
 316 circulatory systems are also frequently affected by the COVID-19, which is aligns with the literature.

This is the author's peer reviewed, accepted manuscript. However, the online version of record will be different from this version once it has been copyedited and typeset.  
PLEASE CITE THIS ARTICLE AS DOI: 10.1063/1.50250923

317 <sup>36-38</sup> Diseases such as 276 (Disorders of fluid electrolyte and acid-base balance), 428 (Heart failure),  
 318 788 (Symptoms involving urinary system), 272 (Disorders of lipid metabolism), 294 (Persistent  
 319 mental disorders due to conditions classified elsewhere) are also more likely to be involved in the  
 320 comorbidity relationships. (Refer to Supplementary Table 3)  
 321



322  
 323 **Figure 2.** Visualization of comorbidity patterns. (A) The comorbidity network. (B) The associations  
 324 among disease groups. In (A), the size of a node is proportional to its occurrence in our dataset. In (B),  
 325 the rectangles in the Sankey diagram correspond to ICD 9 disease categories. The left rectangles



326 represent disease groups of pre-existing diseases. The right rectangles represent disease groups of post-  
327 infection diseases. The edge linking a pair of rectangles indicates that the comorbidity patterns are  
328 significantly more frequent among COVID-19 patients as compared to those in the non-exposed group.  
329 The thickness of an edge is proportional to increased occurrence among COVID-19 patients as  
330 compared to those in the non-exposed group. Please refer to Supplementary Table 5 for more details.

331

332 The comorbidity network's edges suggest more pronounced comorbidity relationships in the exposure  
333 group compared to the non-exposed group. These relationships imply that patients with a history of  
334 respiratory system diseases are at an increased risk of developing further respiratory system diseases  
335 due to COVID-19. Additionally, these patients with a history of respiratory system diseases also  
336 demonstrate a heightened risk for diseases within the circulatory system, genitourinary system, among  
337 others. Patients previously diagnosed with essential hypertension also exhibit a higher risk of  
338 developing respiratory system diseases and lipid disorders due to COVID-19. Patients with a history of  
339 peptic ulcer (site unspecified) are at an increased risk of developing Gastritis and duodenitis (Refer to  
340 Supplementary Table 4).

341

#### 342 **Biological Mechanism Explanation**

343 To investigate the biological mechanisms underlying identified comorbidity relations, we utilize the  
344 PPI and GO terms associated with the diseases. We hypothesize that for COVID-19 to influence the  
345 disease comorbidity patterns of patients, its host factors (genes/proteins) should be localized in the  
346 corresponding subnetwork within the human PPI network, either directly targeting the disease-  
347 associated genes/proteins or indirectly affecting them through PPIs. Specifically, we hypothesize that  
348 these comorbidity patterns identified from the comorbidity network experience a larger reduction in the  
349 topological distance in the PPI network caused by the inclusion of proteins associated with COVID-19  
350 as additional proteins associated with pre-existing disease. Similar patterns were previously observed  
351 in the relationship between COVID-19 and brain microvascular injury.<sup>39</sup>

352



353 After we eliminated disease pairs without associated protein information, 145 pre-existing disease-  
354 post-infection disease pairs, including 84 disease types (74 pre-existing diseases, 37 post-infection  
355 diseases), remained. Then, the network distance from pre-existing diseases to post-infection diseases  
356 is measured on the PPI network. The network distance is measured as the average shortest path length  
357 between each protein associated with post-infection disease and proteins associated with pre-existing  
358 disease. (Equation 3) Next, we measure the change of network distance of pre-existing diseases and  
359 post-infection diseases in the PPI network when treating COVID-19 as an additional pre-existing  
360 disease (Equation 4, Equation 5). We observed that the network distance between the disease pairs  
361 with elevated comorbidity risk after COVID-19 became significantly shorter because of the addition  
362 of proteins associated with COVID-19 in 54 disease pairs among 145 disease pairs (Figure 3). Please  
363 refer to the Method section for details. The result of Wilcoxon signed-rank test about distance change  
364 between exposure and non-exposed groups is shown in Figure 3 (A), Supplementary Figure 2 and  
365 Supplementary Table 6. The result of Z scores about the distance change within exposure groups is  
366 shown in Figure 3 (B), Supplementary Figure 3 and Supplementary Table 7. The sensitivity analysis  
367 is shown in Supplementary Figure 5,6,7 and Supplementary Table 12,13,14,15.

368  
369 Further GO analysis of involved proteins reveals that COVID-19 introduced additional mechanistic  
370 pathways towards post-infection diseases, effectively increasing the risk of developing post-infection  
371 diseases. Please refer to Supplementary Table 8, 9 for a list of frequent GO terms associated with these  
372 proteins.

373  
374 Among the involved proteins, *overlapping* proteins (those associated with both the post-infection  
375 disease and pre-existing disease with COVID-19) play a major role in shortening the distance between  
376 the disease pairs. The distance of each disease pair reflects the likelihood that proteins associated with  
377 post-infection disease are influenced by the abnormal expression of proteins associated with pre-  
378 existing disease with COVID-19 via the PPI network. These proteins representing biological functions  
379 are linked to the phenotype of post-infection disease. For example, in Figure 4, the overlapping proteins  
380 associated with both the post-infection disease (272) and COVID-19 all involved in lipid metabolism,

This is the author's peer reviewed, accepted manuscript. However, the online version of record will be different from this version once it has been copyedited and typeset.  
PLEASE CITE THIS ARTICLE AS DOI: 10.1063/5.0250923

381 the abnormal expression of the proteins may lead to a perturbation of lipid metabolism related biological  
382 functions resulting in the phenotype Disorders of lipid metabolism<sup>40</sup>. Please refer to the Supplementary  
383 Materials for a list of the most frequent overlapping proteins (Refer to Table 2, Supplementary Table  
384 10, 11). GO enrichment analysis reveals that, in addition to the roles in COVID-19 and following  
385 inflammatory response, the expression disorder of these overlapping proteins is leading towards other  
386 diseases involving cardiovascular system, urinary system, and respiratory system.  
387

This is the author's peer reviewed, accepted manuscript. However, the online version of record will be different from this version once it has been copyedited and typeset.  
PLEASE CITE THIS ARTICLE AS DOI: 10.1063/1.50250923



388

389

390

**Figure 3.** Visualization of PPI distance. (A) The distribution of the distance changes from the corresponding disease to other comorbidities in the positive sample and negative sample (including

This is the author's peer reviewed, accepted manuscript. However, the online version of record will be different from this version once it has been copyedited and typeset.  
PLEASE CITE THIS ARTICLE AS DOI: 10.1063/1.50250923

391 significant ( $p < 0.05$ ) disease pairs in Wilcoxon signed-rank test). (B) Z score of comorbidity pairs  
 392 (including significant disease pairs in T test). The bar is thicker, and the Z score is larger. In (A), red  
 393 (blue) rectangles represent pre-existing disease groups in the positive (negative) sample. In (B), each  
 394 bar in the plot represents a comorbidity pair with the wider segment part mapping to the pre-existing  
 395 disease in a disease pair, while the narrower part mapping to the post-infection disease.

396 **Table 2. Top 10 most important overlapping proteins.**

Symbol ID	Type	Associated biological functions
ACE	Enzyme	Involving in blood pressure regulation and electrolyte balance
PDYN	Preproprotein	Proteolytically processing to form the secreted opioid peptides beta-neoendorphin, dynorphin, leu-enkephalin, rimorphin, and leumorphin.
GNAS	Protein	Playing a key role in the classical signal transduction pathway linking receptor-ligand interactions with the activation of adenylyl cyclase and a variety of cellular responses
GSTP1	Enzyme	Playing an important role in detoxification by catalyzing the conjugation of many hydrophobic and electrophilic compounds with reduced glutathione
IL1B	Cytokine	Acting as an important mediator of the inflammatory response, and involving in a variety of cellular activities, including cell proliferation, differentiation, and apoptosis
SCGB1A1	Secreted Proteins	Involved in numerous functions including anti-inflammation, inhibition of phospholipase A2 and the sequestering of hydrophobic ligands
PLAT	Protease	Converting the proenzyme plasminogen to plasmin, a fibrinolytic enzyme
NOS3	Enzyme	Playing an important role in detoxification by catalyzing the conjugation of many hydrophobic and electrophilic compounds with reduced glutathione
HMOX1	Enzyme	Involved in heme catabolism, cleaving heme to form biliverdin
GDF15	Ligand	Acting as a pleiotropic cytokine and participateing in the stress response program of cells after cellular injury. Increased protein levels are associated with disease states such as tissue hypoxia, inflammation, acute injury and oxidative stress.

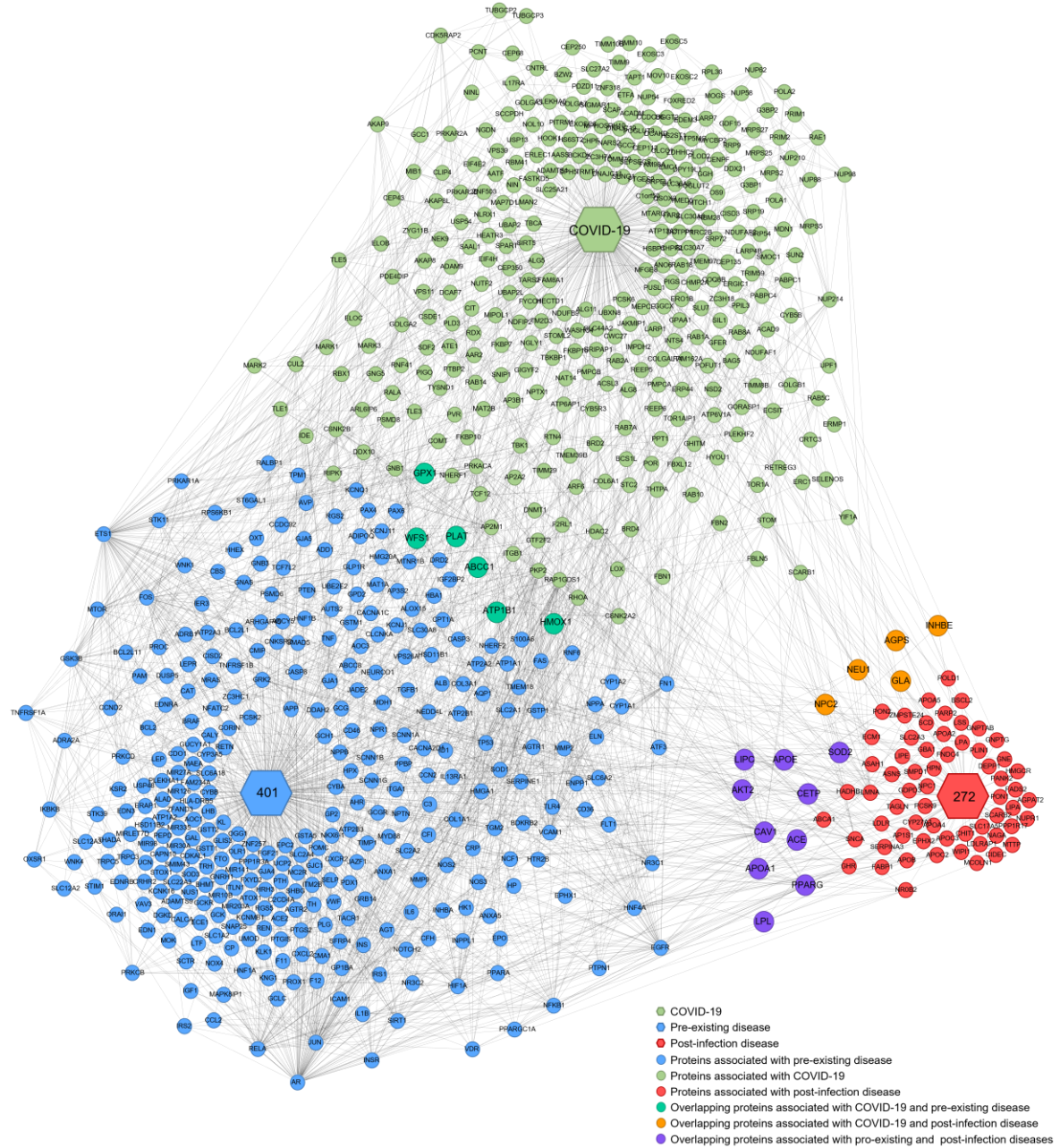
397  
 398 Figure 4 illustrates the interplays between a representative disease comorbidity pair, from 401 (Essential  
 399 hypertension) to 272 (Disorders of lipid metabolism), which has an elevated risk because of the  
 400 COVID-19 infection. We find that the overlapping proteins (orange and purple circles) associated with

This is the author's peer reviewed, accepted manuscript. However, the online version of record will be different from this version once it has been copyedited and typeset.  
PLEASE CITE THIS ARTICLE AS DOI: 10.1063/5.0250923

401 both the post-infection disease (272) and pre-existing diseases (401 and COVID-19) play an important  
402 role in the development of disease comorbidity. There are five additional overlapping proteins (orange  
403 circles) because of the COVID-19 infection: NEU1, INHBE, NPC2, AGPS and GLA.<sup>41,42</sup> Specifically,  
404 NEU1 has a significant effect on lipid metabolism and inflammatory processes and is a potential drug  
405 target for decreasing atherosclerosis.<sup>43,44</sup> INHBE activates energy expenditure through brown/beige  
406 adipocyte activation, and it can be a potential drug target for obesity therapy.<sup>45,46</sup> NPC2 is essential for  
407 the pathways involved in glucose and lipid metabolism, helping the egress of lipids from the lysosome.  
408 <sup>47,48</sup> AGPS is an ether lipid generating enzyme which is important for the balance of structural and  
409 signaling lipids.<sup>49</sup> GLA is a polyunsaturated fatty acid that can reduce lipid deposition.<sup>40</sup> The addition  
410 of these five overlapping proteins representing biological functions related to lipid metabolism  
411 potentially explains the mechanism of how COVID-19 elevated the risk of developing the post-infection  
412 disease (272).  
413  
414



This is the author's peer reviewed, accepted manuscript. However, the online version of record will be different from this version once it has been copyedited and typeset.  
PLEASE CITE THIS ARTICLE AS DOI: 10.1063/1.50250923



415

416

417

418

419

420

**Figure 4. PPIs underlying the comorbidity pattern between ICD 401 and ICD 272.** A hexagon represents a disease. A circle represents a protein. An edge between circles represents the existence of protein-protein interaction. An edge between a hexagon and a circle represents the protein associated with the disease.

421 **DISCUSSION**

422 Our study, leveraging population-based EHR and a wealth of biomedical data, stands as a pioneering  
423 quantitative analysis of the complex molecular mechanisms underlying the comorbidity patterns  
424 associated with COVID-19. This research is not merely an exploration but a comprehensive  
425 examination of the data, aiming to unravel the progression of the disease and the evolution of  
426 comorbidity patterns resulting from a COVID-19 infection.

427 Our findings provide a deeper understanding of the phenomenon known as PASC; a disease  
428 characterized by lingering symptoms after recovery from the acute phase of COVID-19 that has been  
429 a global concern for healthcare professionals. Our research illuminates the elevated-risk comorbidity  
430 patterns associated with PASC, significantly contributing to the existing body of knowledge on this  
431 subject.

432 Central to our study are the key proteins we identified, which play a pivotal role in increasing the risk  
433 of these comorbidity patterns. These proteins are not merely markers but potential targets for therapeutic  
434 intervention, laying the groundwork for the development of new drugs and the repurposing of existing  
435 ones. (More details are shown in Supplementary Table 10, 11) The ultimate goal is not only to reduce  
436 the risk of COVID-19 re-infection but also to prevent the onset of PASC, offering hope to millions of  
437 patients worldwide.

438  
439 The practical applications of our study are extensive. Using the comorbidity patterns, we discovered  
440 and the wealth of data from electronic health records, we can identify patients who are at high risk for  
441 PASC. This information is crucial for the effective allocation of medical resources, ensuring prompt  
442 care for those who need it most. Moreover, it aids in the recovery process of patients from COVID-19,  
443 providing a roadmap for their journey back to health. Our study, therefore, stands at the intersection of  
444 research and real-world application, contributing to the fight against this global pandemic.

445  
446 Our study has limitations. First, our analyses were based on the topology of the PPI network. The PPI  
447 network serves as a “skeleton” of the biological signaling circuitry in the human body. However, PPI



448 network cannot fully represent the pharmacokinetics and pharmacodynamics (PK/PD) associated with  
449 drugs. Future research is needed to incorporate the PK/PD models for a better understanding of the  
450 effects of drugs on the human body. Secondly, our population EHR data was obtained from public  
451 hospitals in Hong Kong. Although our data is among the most complete for a population, there is an  
452 inevitable under-reporting problem, especially for young patients. Third, although we have tried our  
453 best to build a comprehensive mapping between diseases and proteins in the PPI network. The  
454 mapping may still be subject to bias because of the lack of such data. Further biological research is  
455 needed to enrich and complement existing databases. The causative relationship between proteins in  
456 molecular mechanisms remains elusive. Validating these connections necessitates strategic planning  
457 of randomized controlled trials (RCTs) or the application of Mendelian randomization. Additionally,  
458 advanced methodologies in social network<sup>50</sup> and gene regulation network analyses<sup>51-53</sup>, coupled with  
459 the acquisition of supplementary biological datasets, are essential for substantiating these causal  
460 connections.

#### 461 **Conclusions**

462 In conclusion, our study significantly advances the understanding of the intricate molecular mechanisms  
463 and comorbidity patterns associated with COVID-19. By leveraging extensive population-based  
464 electronic health records and biomedical data, we have provided a comprehensive analysis that  
465 elucidates the progression of the disease and the evolution of comorbidity patterns resulting from a  
466 COVID-19 infection. Our findings identify the critical role of specific proteins in increasing the risk of  
467 these comorbidity patterns, identifying them as potential targets for therapeutic intervention. This paves  
468 the way for developing new treatments and repurposing existing drugs, ultimately aiming to reduce the  
469 risk of COVID-19 re-infection and prevent the onset of PASC. The practical implications of our  
470 research are extensive. By identifying high-risk patients through comorbidity patterns and electronic  
471 health record data, we can ensure a more effective allocation of medical resources and provide timely  
472 care to those most in need.

473  
474

475 **Supplementary materials**

476 The supplementary materials contain additional figures and tables of the analytical results.

477

478 **Ethics approval and consent to participate**

479 Ethical approval for this study was granted by the Institutional Review Board of the University of

480 Hong Kong/HA HK West Cluster (UW20-556, UW21-149 and UW21-138).

481

482 **Consent for publication**

483 All authors provide consent for the publication of this manuscript.

484

485 **Competing interests**

486 The authors declare no competing interests.

487

488 **Availability of data and materials**

489 Data and raw code are available at <https://github.com/LueTian/LONG-COVID>. Clinical data

490 could not be deposited for patient privacy reasons.

491

492 **Funding**

493 Research Grants Council of Hong Kong.

494 **Acknowledgements**

495 N/A

496

497 **Authors' Contributions**

498 **T.L.:** methodology, data curation, formal analysis, preparation of the original draft, visualization, data

499 interpretation; **QP:** methodology, data interpretation, writing-review and editing, conceptualization of

500 the project, supervision, acquisition of resources; **EW, SLCC, SL:** writing-review, acquisition of

This is the author's peer reviewed, accepted manuscript. However, the online version of record will be different from this version once it has been copyedited and typeset.  
PLEASE CITE THIS ARTICLE AS DOI: 10.1063/5.0250923

501 resources; **EC**, **HL**: acquisition of resources; **L.C.K.W**: conceptualization of the project, acquisition  
502 of resources.

503

504 **Abbreviations**

505 **PASC**: post-acute sequelae of COVID-19

506 **EHR**: electronic health record

507 **SARS-CoV-2**: severe acute respiratory syndrome coronavirus 2

508 **GO**: Gene Ontology

509 **PPI**: protein-protein interaction

510 **RAT**: rapid antigen test

511 **PCR**: polymerase chain reaction

512 **HKHA**: Hong Kong Hospital Authority

513 **SMD**: standardized mean difference

514 **RR**: Relative Risk

515

516 **REFERENCES**

- 517 1. Davis, H. E., McCorkell, L., Vogel, J. M. & Topol, E. J. Long COVID: major findings,  
518 mechanisms and recommendations. *Nat. Rev. Microbiol.* **21**, 133–146 (2023).
- 519 2. Zhang, H. *et al.* Data-driven identification of post-acute SARS-CoV-2 infection  
520 subphenotypes. *Nat. Med.* **29**, 226–235 (2023).
- 521 3. Russell, C. D., Lone, N. I. & Baillie, J. K. Comorbidities, multimorbidity and COVID-19.  
522 *Nat. Med.* **29**, 334–343 (2023).
- 523 4. Altmann, D. M., Whettlock, E. M., Liu, S., Arachchillage, D. J. & Boyton, R. J. The  
524 immunology of long COVID. *Nat. Rev. Immunol.* **23**, 618–634 (2023).
- 525 5. Xie, Y., Xu, E., Bowe, B. & Al-Aly, Z. Long-term cardiovascular outcomes of COVID-  
526 19. *Nat. Med.* **28**, 583–590 (2022).
- 527 6. Raman, B., Bluemke, D. A., Lüscher, T. F. & Neubauer, S. Long COVID: post-acute  
528 sequelae of COVID-19 with a cardiovascular focus. *Eur. Heart J.* **43**, 1157–1172 (2022).
- 529 7. Xie, Y., Xu, E. & Al-Aly, Z. Risks of mental health outcomes in people with covid-19:  
530 cohort study. *BMJ* **376**, e068993 (2022).
- 531 8. Xie, Y. & Al-Aly, Z. Risks and burdens of incident diabetes in long COVID: a cohort study.  
532 *Lancet Diabetes Endocrinol.* **10**, 311–321 (2022).
- 533 9. Bowe, B., Xie, Y., Xu, E. & Al-Aly, Z. Kidney Outcomes in Long COVID. *J. Am. Soc.*  
534 *Nephrol.* **32**, 2851 (2021).
- 535 10. Su, Y. *et al.* Multiple early factors anticipate post-acute COVID-19 sequelae. *Cell* **185**,  
536 881-895.e20 (2022).

- 537 11. Brodin, P. *et al.* Studying severe long COVID to understand post-infectious disorders  
538 beyond COVID-19. *Nat. Med.* **28**, 879–882 (2022).
- 539 12. Mehandru, S. & Merad, M. Pathological sequelae of long-haul COVID. *Nat. Immunol.* **23**,  
540 194–202 (2022).
- 541 13. Lai, F. T. T. *et al.* Multimorbidity and adverse events of special interest associated with  
542 Covid-19 vaccines in Hong Kong. *Nat. Commun.* **13**, 411 (2022).
- 543 14. Kuan, V. *et al.* Identifying and visualising multimorbidity and comorbidity patterns in  
544 patients in the English National Health Service: a population-based study. *Lancet Digit.*  
545 *Health* **5**, e16–e27 (2023).
- 546 15. Subramanian, A. *et al.* Symptoms and risk factors for long COVID in non-hospitalized  
547 adults. *Nat. Med.* **28**, 1706–1714 (2022).
- 548 16. Ayoubkhani, D. *et al.* Trajectory of long covid symptoms after covid-19 vaccination:  
549 community based cohort study. *BMJ* **377**, e069676 (2022).
- 550 17. Yang, J., Xu, Z., Wu, W. K. K., Chu, Q. & Zhang, Q. GraphSynergy: a network-inspired  
551 deep learning model for anticancer drug combination prediction. *J. Am. Med. Inform. Assoc.*  
552 **28**, 2336–2345 (2021).
- 553 18. Ashburner, M. *et al.* Gene Ontology: tool for the unification of biology. *Nat. Genet.* **25**,  
554 25–29 (2000).
- 555 19. ROSENBAUM, P. R. & RUBIN, D. B. The central role of the propensity score in  
556 observational studies for causal effects. *Biometrika* **70**, 41–55 (1983).

- 557 20. Gomez-Cabrero, D. *et al.* From comorbidities of chronic obstructive pulmonary disease to  
558 identification of shared molecular mechanisms by data integration. *BMC Bioinformatics*  
559 **17**, 441 (2016).
- 560 21. Morselli Gysi, D. *et al.* Network medicine framework for identifying drug-repurposing  
561 opportunities for COVID-19. *Proc. Natl. Acad. Sci.* **118**, e2025581118 (2021).
- 562 22. Gordon, D. E. *et al.* A SARS-CoV-2 protein interaction map reveals targets for drug  
563 repurposing. *Nature* **583**, 459–468 (2020).
- 564 23. Piñero, J. *et al.* The DisGeNET knowledge platform for disease genomics: 2019 update.  
565 *Nucleic Acids Res.* **48**, D845–D855 (2020).
- 566 24. Piñero, J. *et al.* DisGeNET: a comprehensive platform integrating information on human  
567 disease-associated genes and variants. *Nucleic Acids Res.* **45**, D833–D839 (2017).
- 568 25. Hamosh, A., Scott, A. F., Amberger, J. S., Bocchini, C. A. & McKusick, V. A. Online  
569 Mendelian Inheritance in Man (OMIM), a knowledgebase of human genes and genetic  
570 disorders. *Nucleic Acids Res.* **33**, D514–D517 (2005).
- 571 26. Amberger, J. S., Bocchini, C. A., Schiettecatte, F., Scott, A. F. & Hamosh, A. OMIM.org:  
572 Online Mendelian Inheritance in Man (OMIM®), an online catalog of human genes and  
573 genetic disorders. *Nucleic Acids Res.* **43**, D789–D798 (2015).
- 574 27. Klopfenstein, D. V. *et al.* GOATOOLS: A Python library for Gene Ontology analyses. *Sci.*  
575 *Rep.* **8**, 10872 (2018).
- 576 28. Yu, G. *et al.* GOSemSim: an R package for measuring semantic similarity among GO terms  
577 and gene products. *Bioinformatics* **26**, 976–978 (2010).

- 578 29. Yu, G. Gene Ontology Semantic Similarity Analysis Using GOSemSim. in *Stem Cell*  
579 *Transcriptional Networks: Methods and Protocols* (ed. Kidder, B. L.) 207–215 (Springer  
580 US, New York, NY, 2020). doi:10.1007/978-1-0716-0301-7\_11.
- 581 30. Rivals, I., Personnaz, L., Taing, L. & Potier, M.-C. Enrichment or depletion of a GO  
582 category within a class of genes: which test? *Bioinformatics* **23**, 401–407 (2007).
- 583 31. Benjamini, Y. & Hochberg, Y. Controlling the False Discovery Rate: A Practical and  
584 Powerful Approach to Multiple Testing. *J. R. Stat. Soc. Ser. B Methodol.* **57**, 289–300  
585 (1995).
- 586 32. Ramos, J. & others. Using tf-idf to determine word relevance in document queries. in  
587 *Proceedings of the first instructional conference on machine learning* vol. 242 29–48  
588 (Citeseer, 2003).
- 589 33. Xu, Z., Zhang, J., Zhang, Q., Xuan, Q. & Yip, P. S. F. A comorbidity knowledge-aware  
590 model for disease prognostic prediction. *IEEE Trans. Cybern.* **52**, 9809–9819 (2021).
- 591 34. Yu, G., Wang, L.-G., Han, Y. & He, Q.-Y. clusterProfiler: an R Package for Comparing  
592 Biological Themes Among Gene Clusters. *OMICS J. Integr. Biol.* **16**, 284–287 (2012).
- 593 35. Wu, T. *et al.* clusterProfiler 4.0: A universal enrichment tool for interpreting omics data.  
594 *The Innovation* **2**, 100141 (2021).
- 595 36. Borczuk, A. C. & Yantiss, R. K. The pathogenesis of coronavirus-19 disease. *J. Biomed.*  
596 *Sci.* **29**, 87 (2022).



- 597 37. van Doorn, A. S., Meijer, B., Frampton, C. M. A., Barclay, M. L. & de Boer, N. K. H.  
598 Systematic review with meta-analysis: SARS-CoV-2 stool testing and the potential for  
599 faecal-oral transmission. *Aliment. Pharmacol. Ther.* **52**, 1276–1288 (2020).
- 600 38. Xiao, F. *et al.* Evidence for Gastrointestinal Infection of SARS-CoV-2. *Gastroenterology*  
601 **158**, 1831-1833.e3 (2020).
- 602 39. Zhou, Y. *et al.* Network medicine links SARS-CoV-2/COVID-19 infection to brain  
603 microvascular injury and neuroinflammation in dementia-like cognitive impairment.  
604 *Alzheimers Res. Ther.* **13**, 110 (2021).
- 605 40. Liang, Y. *et al.*  $\gamma$ -Linolenic Acid Prevents Lipid Metabolism Disorder in Palmitic Acid-  
606 Treated Alpha Mouse Liver-12 Cells by Balancing Autophagy and Apoptosis via the  
607 LKB1-AMPK-mTOR Pathway. *J. Agric. Food Chem.* **69**, 8257–8267 (2021).
- 608 41. Yang, D. *et al.* Targeting intracellular Neu1 for coronavirus infection treatment. *iScience*  
609 **26**, 106037 (2023).
- 610 42. Satu, M. S. *et al.* Disease and comorbidities complexities of SARS-CoV-2 infection  
611 with common malignant diseases. *Brief. Bioinform.* **22**, 1415–1429 (2021).
- 612 43. White, E. J. *et al.* Sialidase down-regulation reduces non-HDL cholesterol, inhibits  
613 leukocyte transmigration, and attenuates atherosclerosis in ApoE knockout mice. *J. Biol.*  
614 *Chem.* **293**, 14689–14706 (2018).
- 615 44. Zhang, C., Chen, J., Liu, Y. & Xu, D. Sialic acid metabolism as a potential therapeutic  
616 target of atherosclerosis. *Lipids Health Dis.* **18**, 173 (2019).

- 617 45. Jensen-Cody, S. O. & Potthoff, M. J. Hepatokines and metabolism: Deciphering  
618 communication from the liver. *Mol. Metab.* **44**, 101138 (2021).
- 619 46. Sekiyama, K., Ushiro, Y., Kurisaki, A., Funaba, M. & Hashimoto, O. Activin E enhances  
620 insulin sensitivity and thermogenesis by activating brown/beige adipocytes. *J. Vet. Med.*  
621 *Sci.* **81**, 646–652 (2019).
- 622 47. Gu, J. *et al.* The role of lysosomal membrane proteins in glucose and lipid metabolism.  
623 *FASEB J.* **35**, e21848 (2021).
- 624 48. Sleat, D. E. *et al.* Genetic evidence for nonredundant functional cooperativity between  
625 NPC1 and NPC2 in lipid transport. *Proc. Natl. Acad. Sci.* **101**, 5886–5891 (2004).
- 626 49. Benjamin, D. I. *et al.* Ether lipid generating enzyme AGPS alters the balance of structural  
627 and signaling lipids to fuel cancer pathogenicity. *Proc. Natl. Acad. Sci.* **110**, 14912–14917  
628 (2013).
- 629 50. Ogburn, E. L., Sofrygin, O., Díaz, I. & van der Laan, M. J. Causal Inference for Social  
630 Network Data. *J. Am. Stat. Assoc.* **119**, 597–611 (2024).
- 631 51. Bang, S., Kim, J.-H. & Shin, H. Causality modeling for directed disease network.  
632 *Bioinformatics* **32**, i437–i444 (2016).
- 633 52. Feuerriegel, S. *et al.* Causal machine learning for predicting treatment outcomes. *Nat. Med.*  
634 **30**, 958–968 (2024).
- 635 53. Belyaeva, A., Squires, C. & Uhler, C. DCI: learning causal differences between gene  
636 regulatory networks. *Bioinformatics* **37**, 3067–3069 (2021).
- 637
- 638